IJSES
Volume 9, Issue 4, pp. 86-94, 2025.
International Journal of Scientific Engineering and Science
ISSN (Online): 2456-7361

The Dolerites of the Mayo Oulo-Léré and Babouri-Figuil Cretaceous Basins (North Cameroon and Southwestern Chad, Africa): New Insights

Jean-Paul Vicat[1], Jean-Claude Doumnang Mbaigané[1]
[1]Laboratory of Geology, Geomorphology, and Remote Sensing, Faculty of Exact and Applied Sciences, University of N'Djamena, P.O. box 1027, N'Djamena, Republic of Chad
Email address: jpvicat@gmail.com

Abstract*— This study revisits the chemical composition and geotectonic context of previously analysed dolerites from the Mayo Oulo-Léré and Babouri-Figuil cretaceous Basins. The dolerites are reclassified into initial rifting tholeiites (IRT), continental tholeiites (CT), transitional basalts, and alkaline dolerites. Mapping reveals that IRT are confined to the Mayo Oulo-Léré Basin, while CT and transitional dolerites are restricted to the Proterozoic basement. Alkaline dolerites occur in both the Cretaceous basins and the Proterozoic basement. Geochemical data indicate that the Cretaceous alkaline dolerites derive from an OIB-type mantle source, whereas other dolerites originate from a source intermediate between OIB and E-MORB. CT are associated with a spinel-bearing mantle source, while other dolerites are linked to a garnet-bearing mantle. IRT and alkaline dolerites originate from an asthenospheric source, whereas CT and transitional dolerites reflect a mixed lithospheric-asthenospheric source. Depth estimates from FractionatePT software indicate magma segregation at depths ranging from 49 to 105 km, consistent with asthenospheric upwelling during Cretaceous rifting. While the lack of radiometric dating limits precise age determination, field evidences proves that IRT and alkaline dolerites were emplaced during Cretaceous period. Transitional dolerites may correspond to earlier volcanic activity of the Cameroon Volcanic Line, whereas CT are likely of Paleozoic to early Mesozoic age. These results provide a refined understanding of the magmatic and tectonic history of the Mayo Oulo-Léré and Babouri-Figuil Basins.*

Keywords*— Cretaceous basins of Mayo Oulo-Léré and Babouri-Figuil, Cameroon, Chad, dolerites.*

I. INTRODUCTION

The Mayo Oulo-Léré Basin (MOLB) and the Babouri-Figuil Basin (BFB) are small Cretaceous basins located northeast of the Yola-Guéra branch, which marks the easternmost extension of the Benue Trough (Fig. 1). The MOLB consists of the Mayo Oulo Basin in Cameroon and its extension, the Léré Basin, in Chad. The BFB is entirely situated in Cameroon. Other small Cretaceous basins, including Hama Koussou, Koum, Lamé, Vina, Babouan, Djérem, and Mberé, are also present in Cameroon (Fig. 1). To the southwest of Chad, the Pala and Lamé basins represent the western extensions of the Bongor and Doba basins, which are largely covered by Quaternary deposits (Fig. 1). These Cretaceous basins, along with the large Benue Trough, form part of the West and Central African Rift System (WCARS) (Fig. 1) attributed to the opening of the Southern Atlantic Ocean (Genik, 1992; Guiraud et al., 1992; Guiraud and Maurin, 1992).

The basement in this region, composed of Proterozoic metamorphic and magmatic rocks, belongs to the Pan-African Central African Fold Belt (Bessoles and Trompette, 1980). This fold belt was formed approximately 600 million years ago through the collision between the Congo and West African cratons (Castaing et al., 1994; Toteu et al., 2004).

The MOLB and BFB were initially studied by Schwoerer (1965) in Cameroon, as well as Wacrenier (1962) and Wolff (1964) in Chad. The MOLB was later mapped by Isseini (2011). In this region, where outcrops are often covered by Quaternary deposits, this mapping has been used in several subsequent studies (Klamadji et al., 2020, 2021; Nkouandou et al., 2022; Gountié Dedzo et al., 2023). More detailed mapping has been conducted for the Léré area in Chad (Doumnang Mbaigané, 2006; Doumnang Mbaigané et al., 2025) and for the Mayo Oulo and Figuil basins in Cameroon (Fosso Menkem et al., 2024).

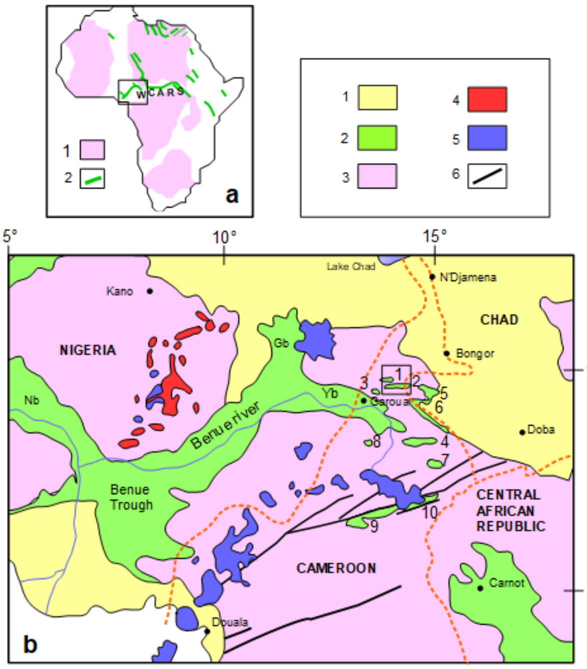

Fig. 1. (a) Distribution of cratons and Mesozoic rifts in Africa. 1: Cratons. 2: Mesozoic rifts. WCARS: West and Central African rifts system. Inset: Location of Fig. b. (b) Geological sketch map of the Benue Trough. Nb, Niger branch; Yb, Yola branc; Gb, Gongola branch. 1: Quaternary sediments. 2: Cretaceous to Tertiary sediments. 3: Proterozoic basement. 4: Jurassic ring

International Journal of Scientific Engineering and Science
Volume 9, Issue 4, pp. 86-94, 2025. ISSN (Online): 2456-7361

complexes. 5: Cenozoic to recent magmatism of the Cameroon Line. Cretaceous basins of Northern Cameroon and Chad: 1, Figuil; 2, Mayo Oulo (Cameroon)–Léré (Chad); 3, Hama Koussou; 4, Koum; 5, Pala; 6, Lamé; 7, Vina; 8, Babouan; 9, Djérem; 10, Mberé. Inset: location of Fig. 2.

Numerous dolerite dykes crosscut the Cretaceous basins of the MOLB and BFB, as well as the Proterozoic basement. These dolerites have been the subject of several studies (Ngounounou et al., 2001; Doumnang Mbaigané, 2006; Klamadji et al., 2020, 2021, 2025; Nkouandou et al., 2022; Gountié Dedzo et al., 2023; Doumnang Mbaigané et al., 2025). They have been attributed to either tholeiitic or alkaline magmatism. In Chad, in the Léré region, Doumnang Mbaigané (2006) and Doumnang Mbaigané et al., (2025) distinguish between dolerites with initial rift tholeiite (IRT) or alkaline basalt compositions associated with the Léré Cretaceous basin, and dolerites with continental tholeiite (CT), transitional basalt, or alkaline compositions that crosscut the basement.

In this paper, we re-examine the chemical compositions of dolerite analyses available in the literature to differentiate dolerites based on their geotectonic context. We present a schematic map of the MOLB and BFB region, distinguishing between IRT, CT, alkaline dolerites, and transitional dolerites. Furthermore, we specify the source and depth of the primary magmas. Lastly, we reflect on the age of the dolerites that crosscut the Pan-African basement.

II. Geological Setting

The MOLB (Fig.2) extending over 50 km with a maximum width of 10 km and a sediment thickness reaching 2.5 km (Bessong et al., 2018) is an asymmetrical syn-sedimentary E-W syncline superimposed on half graben structure. Its asymmetry is due to major normal faults located along the southern edge, formed during the basin's progressive infilling (Maurin and Guiraud, 1989, 1990; Fosso Menkem, 2024). The sedimentary sequence begins with conglomerates and coarse sandstones, followed by a thick succession of alternating sandstones, marlstones, shales, and carbonates (Tchouatcha et al., 2021a, b). These deposits, of fluviolacustrine origin, reflect varied climatic conditions, with more humid settings at the base and more arid conditions towards the top (Bessong et al., 2018; Ngo Elogan Ntem et al., 2024). Fossils found in the middle part of the series indicate Barremian sedimentation (Brunet et al., 1988), while the lower levels are dated to the Valanginian–Hauterivian transition (Ndjeng, 1992). In the upper levels, the presence of Monoporopollenites annulatus suggests a Tertiary age (Eocene or younger) or modern contamination (Bessong et al., 2018).

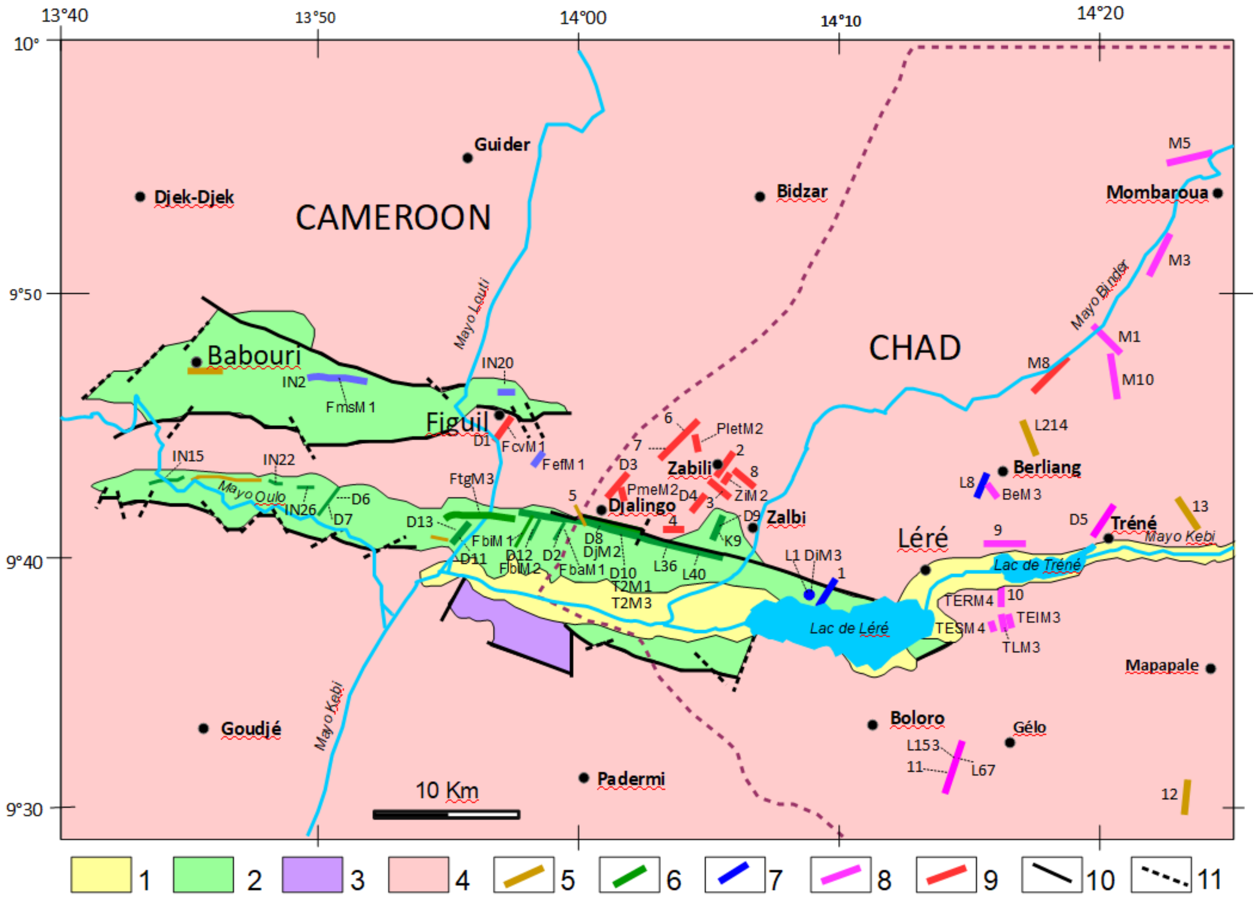

Fig.2. Simplified geological map of the Mayo Oulo-Léré and Babouri-Figuil basins. Modified from Doumnang Mbaigané (1986), Isseini et al,. (2012), Ngounouno et al,. (2001), Klamadji et al,. (2020, 2021), Nkouandou et al,. (2022), Gountié Dedzo et al,. (2023), Fosso Menkem et al,. (2024), Doumang et al,. (2025), and Google Earth satellite imagery. 1: Quaternary sediments. 2: Cretaceous to Tertiary sediments. 3: Mangbai Paleozoic graben 4: Proterozoic basement. 5-9: Dolerite dykes, (5: Unspecified magmatic affinity. 6: Initial Rift Tholeiites. 7: Alkaline. 8: Transitional. 9: Continental Tholeiites). 10: Normal major faults. 11: Transverse minor fault.

International Journal of Scientific Engineering and Science
Volume 9, Issue 4, pp. 86-94, 2025. ISSN (Online): 2456-7361

The BFB (Fig. 2) extends in an E-W direction over 33 km with a maximum width of 7.5 km (Ndjeng, 1992). The thickness of the sedimentary series could reach up to 1500 m (Schwoerer, 1965). It exhibits the same half-graben structure as the MOLB (Maurin and Guiraud, 1989, 1990; Fosso Menkem et al., 2024). The sedimentary sequence begins with breccias, conglomerates, and sandstones, followed by rhythmic sedimentation characterized by regular interbedding of clay, siltstone, shale, and sandstone (Ndjeng, 1992), deposited in a lacustrine, fluvial, and deltaic environment (Nyangono Abolo et al., 2014; Bessong et al., 2018). Fossil vertebrates, petrified wood, and ostracods suggest an Early Cretaceous (Barremian-Aptian) age (Jacobs et al., 1988), while pollen assemblages strongly indicate a Cenomanian-Turonian age for the uppermost levels (Bessong et al., 2018).

Most of the deformation observed in the MOLB and BFB is synsedimentary (Maurin and Guiraud, 1990; Manga Owona et al., 2023; Fosso Menkem et al., 2024). Minor post-sedimentary deformations indicate a N-S shortening direction (Maurin and Guiraud, 1990). This tectonic event is associated with the Santonian compressional episode described in the Benue Trough (Benkhelil, 1986) and also with late Eocene compression (Guiraud et al., 1987; Guiraud and Bellion, 1995).

The MOLB and BFB region is intruded by dolerite dykes oriented N0° to N15°E, N40°E to N65°E, and N100°E to N160°E, which correspond to the direction of Precambrian faults (Maurin and Guiraud, 1990, 1993; Ngounouno et al., 2001).

The dolerite dykes exhibit various textures typical of dolerites, including ophitic, sub-ophitic, doleritic, and intersertal textures. In some cases, their structures resemble those of gabbros. Their mineralogical composition consists of plagioclase, clinopyroxene, opaques, ± olivine, ± orthopyroxene, ± alkali feldspar, ± amphibole, ± biotite, ± apatite, ± titanite as primary minerals, and secondary minerals such as ± epidote, ± chlorite, ± sulfides, and ± calcite. These dolerites evolved through limited fractional crystallization, accompanied for the most part by minor assimilation processes.

There is no radiometric dating available for the basic magmatism of the MOLB and BFB. Pillow basalts are observed near the base of the MOLB sequence (Brunet et al., 1988) and within the BFB (Manga Owona, 2023; Fosso Menkem et al., 2024). Sills and dykes of dolerites and basalts, with contact metamorphism at their margins, have been documented in the MOLB (Brunet et al., 1988; Ndjeng, 1992; Fosso Menkem et al., 2024) and the BFB (Manga Owona, 2023; Fosso Menkem et al., 2024). The basic magmatism in the MOLB and BFB is therefore of syn-Cretaceous to post-Cretaceous age. Structural field data indicate that the doleritic dykes are older than the regional compressive event of the Late Eocene (Guiraud et al., 1987; Guiraud and Bellion, 1995).

The dykes that crosscut the Proterozoic basement have not been dated but are attributed to an extensional tectonic phase during the Paleozoic to Early Mesozoic (Doumnang Mbaigané, 2006; Fagny Mefire et al., 2019; Gountié Dedzo et al., 2023).

III. Methods

We re-examine the geochemical compositions of dolerites from the literature (Ngounouno et al., 2001; Doumnang Mbaigané, 2006; Klamadji et al., 2020, 2021, 2025; Nkouandou et al., 2022; Gountié Dedzo et al., 2023; Doumnang Mbaigané et al., 2025). Magmatic affinity is determined using TAS (Le Bas et al., 1986), Zr/Ti vs. Nb/Y (Winchester and Floyd 1977), and FeO/MgO vs. SiO_2 (Miyashiro, 1975) diagrams. The geotectonic setting is assessed from mantle-normalized incompatible element patterns and the Cabanis and Lecolle (1989) diagram. We provide a schematic geological map of the MOLB and BFB regions (Fig. 2) differentiating the dolerite types (IRT, CT, alkaline and transitional) to illustrate their spatial distribution. Magma sources and melt segregation depths are constrained using Th/Yb vs. Nb/Yb (Pearce, 2008), $(Tb/Yb)_N$ vs. $(La/Yb)_N$ (Wang et al., 2002), Nb/La vs. La/Yb (Smith et al., 1999), and the FractionatePT software of Lee et al., (2009). We also discuss the age of dolerites intruding the Proterozoic basement by comparing their compositions with basic intrusions from northern Cameroon and southern Chad, where geochemical data and, in some cases, ages are available.

IV. Results and Discussion

A. *Geotectonic affinity*

In the TAS diagram (Le Bas et al., 1986) (Fig. 3), the dolerites of the MOLB can be classified as basalts and basaltic andesites. The dolerites of the BFB are trachyandesites and trachytes. The dolerites that crosscut the Pan-African basement are predominantly basalts and trachybasalts, with one sample classified as a trachyandesite. Most of the dolerites from the MOLB basin plot under the subalkaline-alkaline boundary defined by Irvine and Baragar (1971). In contrast, most dolerites associated with the Pan-African basement plot above or near this boundary.

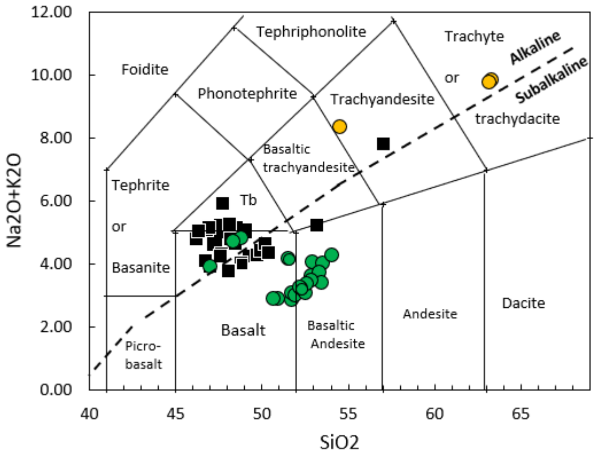

Fig. 3. Chemical compositions of dolerites plotted on the Total Alkali-Silica (TAS) diagram (wt% volatile-free recalculated compositions) (Bas et al., 1986). The dotted line represents the boundary between the tholeiitic and alkaline fields as defined by Irvine and Baragar (1971). Tb: Trachybasalt. Green circles: dolerites from the Mayo Oulo-Léré Basin. Orange circles: dolerites from the Babouri-Figuil Basin. Black squares: dolerites from the basement.

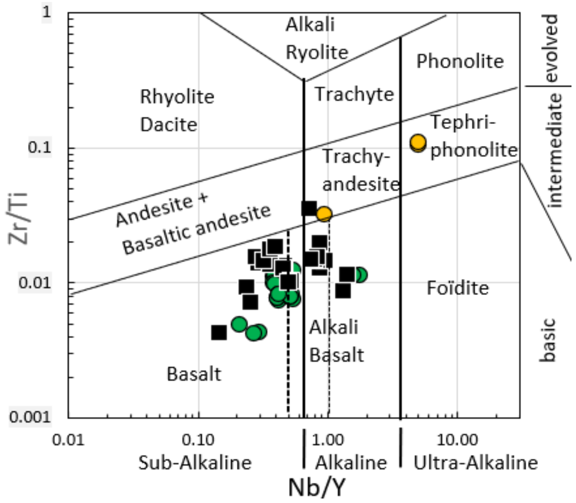

Fig. 4. Zr/Ti vs. Nb/Y diagram (Winchester and Floyd, 1977) modified par Pearce (1996). The dotted black lines delineate the field of transitional basalts according to Pearce and Cann (1973). Same legend as Fig. 2.

The dolerites of the MOLB and BFB are more or less altered, with the formation of secondary minerals, which may have affected the concentrations of highly mobile elements such as Na and K. Consequently, we examine the chemical composition of the dolerites using the Zr/Ti vs. Nb/Y diagram (Winchester and Floyd, 1977) (Fig. 3) based on immobile elements. This diagram confirms that the dolerites of the MOLB are predominantly sub-alkaline, with only two samples classified as alkaline. The dolerites associated with the Pan-African basement are either sub-alkaline or alkaline. According to Pearce and Cann (1973), most of the alkaline dolerites are transitional (Nb/Y < 1), with only two samples being truly alkaline (Nb/Y > 1).

To differentiate subalkaline dolerites the FeO/MgO vs SiO_2 diagram (Miyashiro, 1975) (Fig. 5) is preferred over the AFM diagram (Irvine and Baragar, 1971) due to the mobility of Na and K. In this diagram, all the subalkaline samples from Fig. 4 plot within the tholeiitic field.

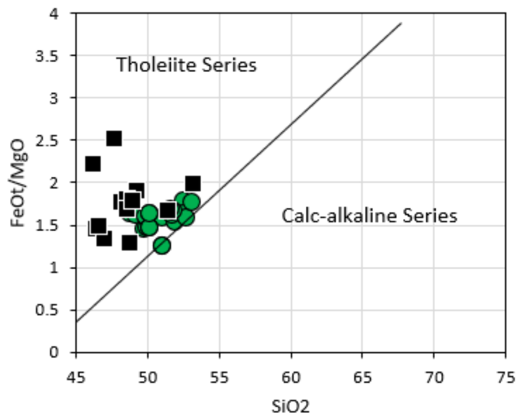

Fig. 5. FeO/MgO vs. SiO_2 diagram after Miyashiro (1975). FeO is total iron. Same legend as Fig. 2.

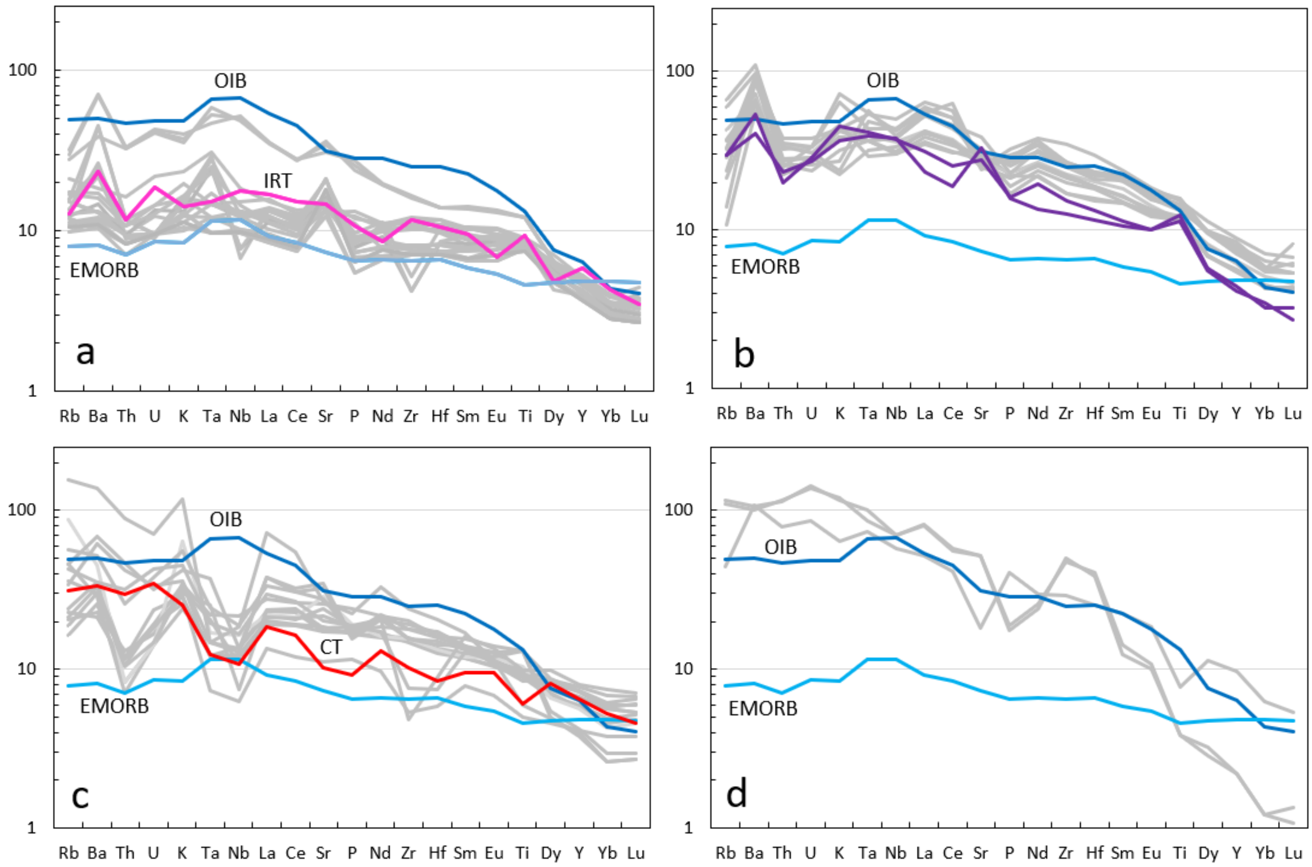

Fig. 6. Primitive mantle-normalized trace element diagrams for the dolerites. Normalization values, OIB, and E-MORB from Sun and McDonough (1989). 6a: Dolerites from the MOLB with tholeiitic and alkaline compositions; IRT after Holm (1985) and Alvaro et al., (2014) for Ta, Nd, Eu, Dy, and Lu. 6b: Dolerites

International Journal of Scientific Engineering and Science
Volume 9, Issue 4, pp. 86-94, 2025. ISSN (Online): 2456-7361

from the Proterozoic basement with transitional and alkaline (purple curves) compositions. 6c: Dolerites from the Proterozoic basement with tholeiitic compositions; CT after Holm (1985). 6d: Alkaline dolerites from the BFB.

We use the incompatible element profiles to determine the geotectonic signature of the dolerites. The multi-element diagrams, normalized to the primitive mantle of Sun and McDonough (1989) (Fig. 6), show varied profiles with enrichment in the most incompatible elements and depletion in the least incompatible elements.

Alkali dolerites of the MOLB (Fig 6a) show profiles similar to those of OIB with significant enrichment in Nb and Ta (Nb_N/La_N=1.39–1.46; Ta_N/La_N=1.32–1.69) consistent with values reported for OIB (Nb_N/La_N=1.25; Ta_N/La_N=1.22) (Sun and McDonough, 1989). Tholeiitic dolerites of MOLB (Fig 6a) display profiles close to EMORB and are comparable to IRT of Holm (1985). The two alkaline dolerites from the basement (Fig. 6b) have profiles similar to those of the alkaline dolerites of MOLB (Fig 6a). The transitional dolerites (Fig. 6b) display profiles similar to those of OIB; however, an OIB-like source is not supported by the negative Nb and Ta anomalies (mean Nb_N/La_N = 0.78; mean Ta_N/La_N=0.86).

The tholeiites from the basement (Fig. 6c) display characteristic CT profiles, with varying degrees of differentiation, a significant negative Nb-Ta anomaly and highly variable Th concentrations. The alkaline dolerites from Figuil (Fig. 6d) exhibit steep negative slopes from Rb to Yb. These include one camptonite with an OIB-like profile and two benmoreites highly depleted in heavy rare earth elements (Ngounouno et al., 2001; Klamadji et al., 2021).

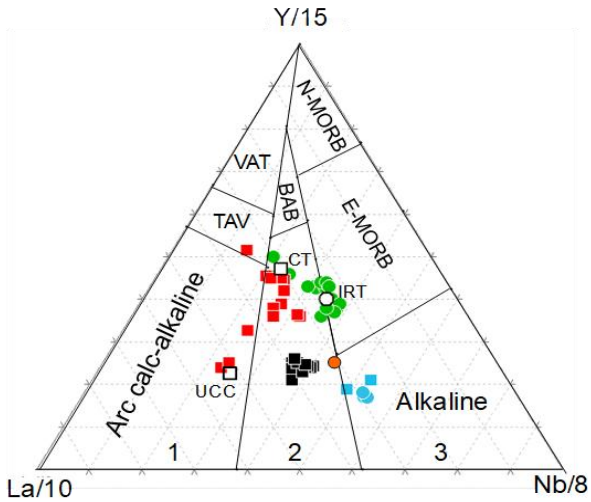

Fig. 7. Plot of dolerites in the Cabanis and Lécolle (1989) diagram. Differentiated dolerites with SiO_2 (anhydrous weight) > 55% are excluded. 1: Orogenic domain. 2: Late to post-orogenic compressive to distensive intra-continental domain. 3: Anorogenic distensive domain. VAT: Volcanic arc tholeiites. TAV: Transitional arc volcanism. BAB: Back arc volcanism. CT and IRT after Holm (1985). Upper continental crust (UCC) composition after Rudnick and Gao (2004). Dolerites from the MOLB: blue circles, alkaline dolerites; green circles, IRT. Dolerites from the basement: blue squares, alkaline dolerites; black squares, transitional dolerites; red squares, CT. Dolerite for the BFB : orange circle.

The geotectonic signatures of the dolerites are supported by their distribution in the La-Y-Nb diagram (Cabanis and Lécolle, 1989). Most of the dolerites from the MOLB plot near the IRT field of Holm (1985), which forms during lithospheric thinning associated with rift formation. The crustal thinning allows the upwelling of the asthenosphere and its melting by adiabatic decompression. The alkaline dolerites of the MOLB and the Proterozoic basement plot in the alkaline field. The tholeiitic and transitional dolerites of the Proterozoic basement plot within the intra-continental field, as the CT of Holm (1985). The camptonite of the BFB lies at the boundary between the alkaline and intra-continental fields.

In this diagram, crustal contamination shifts the sample points toward the orogenic field due to Nb depletion. Consequently, some CT samples are displaced into the orogenic domain, with two highly contaminated samples positioned near the Upper Continental Crust, while a few IRT samples are shifted toward the CT field.

B. Cartography

The Fig. 2 presents a simplified geological map of the MOLB and BFB. The dolerites are categorized based on their geotectonic signature:

- Alkaline dolerite : samples IN20, IN2 after Ngounouno et al., (2001), FefM1 after Klamadji et al., (2020), FmsM1, DiM3 after Klamadji et al., (2021), 1 after Nkouandou et al., (2022), and L1, L8 after Doumnang Mbaigané et al., (2025),
- IRT : samples IN15, IN22, IN26 after Ngounounou et al., (2001), ZaM1, T2M3, T2M1, DJM2, FtgM3 after Klamadji et al., (2021), D2, D6, D7, D8, D9, D10, D11, D12, D13 after Gountié Dedzo et al., (2023), L36 , L40 after Doumnang Mbaigané et al., (2025), and FbiM1, FbaM1, FbiM2 after Klamandji et al., 2025,
- Transitional dolerite : samples TESM4, TEIM3, TERM4, TLM3, BeM3 after Klamandji et al., (2020), 10 , 9 after Nkouandou et al., (2022), D5 after Gountié Dedzo et al,. (2023), and M10, L67, M3, M5, M1 after Doumnang Mbaigané et al., (2025),
- CT : samples ZiM2, PmeM2, FcvM1, PletM2 after Klamadji et al., (2020), 2, 3, 4, 6, 7, 8 after Nkouandou et al., (2022), D1, D3, D4 after Gountié Dedzo et al., (2023), and M8 after Doumnang Mbaigané et al., (2025).

CT and transitional dykes are restricted to the Proterozoic basement (Fig. 2), while IRT occur exclusively within the MOLB. Alkaline dolerites are less common, with two dykes located at the eastern end of the MOLB, three within the BFB, and two others crosscutting the Proterozoic basement.

C. Source of Magmas and Depth of Melt Segregation

In the Th/Yb vs Nb/Yb diagram (Pearce, 2008) (Fig. 8), several distinct sources are identified. The alkaline Cretaceous dolerites of the MOLB originate from an OIB-type mantle source. The other dolerites come from an intermediate source between OIB and E-MORB. The tholeiitic dolerites are sometimes affected by slight crustal contamination and consequently plot near the CT of Holm (1985). The two samples strongly affected by crustal contamination (see Fig. 7) are shifted toward the field of active continental margin basalts. The Cretaceous dolerites with IRT composition plot near the

International Journal of Scientific Engineering and Science
Volume 9, Issue 4, pp. 86-94, 2025. ISSN (Online): 2456-7361

IRT field of Holm (1985). Three IRT samples show slight crustal contamination.

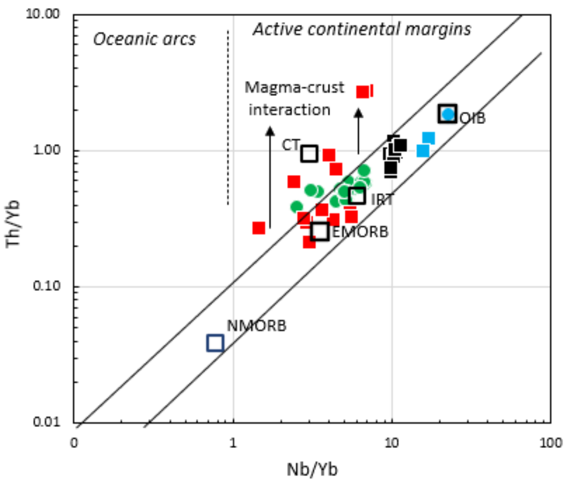

Fig. 8. Plot of dolerites in the Th/Yb vs. Nb/Yb diagram (Pearce, 2008). Differentiated dolerites (SiO_2 anhydrous weight > 55%) are excluded. Symbols as in Fig 7.

A garnet-bearing source is suspected if the Tb/Yb ratio normalized to Primitive Mantle is greater than 1.8 (Wang et al., 2002) or if Gd/Yb normalized to C1 chondrite is greater than 2 (Rooney, 2010). In the (Tb/Yb)N vs. (La/Yb)N diagram (Fig.9) after Wang et al., (2002), CT originates from a spinel-bearing mantle source, while the other dolerites originate from a garnet-bearing source. The Gd/Yb vs. La/Sm diagram (Rooney, 2010), not shown here, leads to the same conclusion.

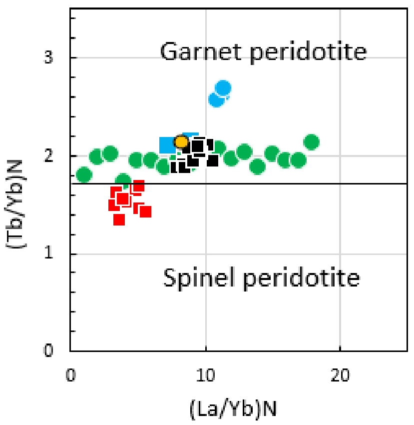

Fig. 9. (Tb/Yb)N versus (La/Yb)N plot of MOLB and BFB dolerites after Wang et al., (2002). Tb, La, and Yb are normalized to Primitive Mantle from McDonough and Sun (1995). The two strongly contaminated dolerites and differentiated dolerites (SiO_2 anhydrous weight > 55%) are excluded. Symbols as in Fig 7.

The asthenospheric mantle is HFSE-enriched and HREE-depleted compared to the lithospheric mantle (Smith et al., 1999). Therefore, high Nb/La ratios are characteristic of magmas derived from the asthenospheric mantle, whereas lower Nb/La ratios indicate derivation from the lithospheric mantle. In the Nb/La vs. La/Yb diagram after Smith et al., (1999) (Fig. 10), the alkaline and IRT dolerites exhibit high Nb/La ratios greater than 1, indicating an asthenospheric source. The contaminated IRT samples are shifted into the mixed domain due to their depletion in Nb. The transitional dolerites and CT display low Nb/La ratios, less than 1, suggesting a mixed asthenospheric-lithospheric mantle source.

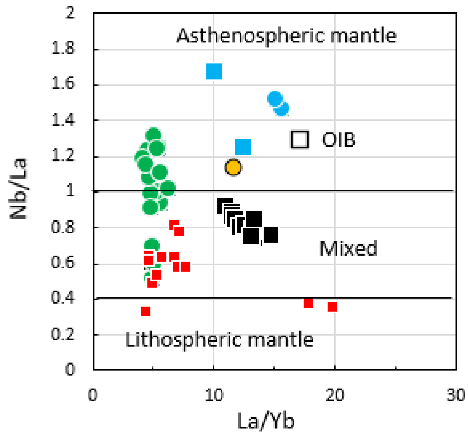

Fig. 10. Plot of MOLB and BFB dolerites in the Nb/La vs La/Yb diagram after Smith et al., (1999). Symbols as in Fig 7.

The calculation of primary magma formation with the FractionatePT software of Lee et al., (2009) for samples with MgO > 6.5% yields a mean pressure of 1.64 GPa for the IRT, 2.50 GPa for the Cretaceous alkaline dolerites of the MOLB and BFB, 3.28 GPa for the alkaline dolerites of the basement, 3.51 GPa for the transitional dolerites, and 2.40 GPa for the CT. Considering 1 GPa = 30 km, this corresponds to a mean depth of 49 km for the IRT, 75 km for the Cretaceous alkaline dolerites of the MOLB and BFB, 98 km for the alkaline dolerites of the basement, 105 km for the transitional dolerites, and 72 km for the CT.

Although this software slightly underestimates the pressures for non-primary basalts, the shallow origin depths of the IRT, compared to the other dolerites, confirm the upwelling of the asthenosphere beneath the MOLB and BFB.

D. Regional Implications and Reflections on the age of the dolerites

The IRT and the alkaline dolerites of the MOLB and BFB basins have not been directly dated. Their emplacement age, ranging from syn-Cretaceous to post-Cretaceous and predating the end of the Eocene, is constrained by field evidence. Regionally, this period is marked by magmatic activity associated with the functioning of the WCARS. To the west, in Nigeria, basalts from the Benue Trough (Coulon et al., 1996), which have a composition similar to the dolerites of the MOLB have been dated by K-Ar between 147 and 49 Ma (Maluski, 1995). In northern Cameroon and southwestern Chad, basaltic dykes have K-Ar ages ranging from 87 to 43 Ma (Wilson et al., 2014). In Chad, doleritic sills from the Bongor Basin have been dated by K-Ar at 67.5–51.9 Ma (Lu et al., 2009a, b) and 56–52 Ma (Genik, 1992), while tholeiitic basalts have been dated to the Barremian (Lu et al., 2009a, b). Basaltic sills have been dated by K-Ar at 95–75 Ma in the Doba Basin (Dou et al., 2023) and 101–97 Ma in the Dosseo Basin (Genik, 1992). These ages are consistent with the activity of the MOLB and BFB basins from the Neocomian to the Eocene. The two alkaline dolerites that crosscut the Proterozoic basement are likely contemporaneous with the alkaline dolerites of the MOLB and BFB.

In Cameroon, numerous basic dykes with CT composition crosscut the Pan-African basement (Béa et al., 1990; Vicat et al., 2001; Kouankap Nono et al., 2013; Nkouandou et al., 2017; Tchaptchet Tchato et al., 2017; Aka et al., 2018; Fagny Mefire et al., 2019; Kuetchafo Kouamo et al., 2019; Okomo Atoumba et al., 2021; Assah et al., 2022; Lemdjou et al., 2022). These dykes are sometimes overlain by the recent volcanism of the Cameroon Line (CL). They cannot be associated with the basic volcanism of the Benue Rift, whose composition is either alkaline or tholeiitic, similar to the IRT (Coulon et al., 1996). Therefore, the CT dykes must be at least older than the Upper Jurassic. The CT dykes of the Mangbai Graben, located immediately south of the MOLB (Fig. 2), have been dated by K-Ar at 384 ± 11 Ma and 425 ± 12 Ma (Lasserre et al., 1977). Further west, in Cameroon, the few available CT datings indicate Ordovician ages for the dolerites of Kekem (Lemdjou et al., 2022) and Triassic ages for the dolerites of Bafoussam (Kouankap Nono et al., 2013) and Nyos (Aka et al., 2018). The CT of the MOLB and BFB region are thus very likely of Paleozoic to early Mesozoic age.

The transitional dolerites that intrude the basement in the MOLB and BFB region have compositions distinct from the basic volcanism—either alkaline or tholeiitic—of the Benue Trough (Coulon et al., 1996). Transitional basic dykes also crosscut the Pan-African basement in Cameroon, notably at Bafoussam (Kouankap Nono et al., 2013), Foumban and Nyos (Asaah et al., 2022), and Manjo (Kuetchafo Kouamo et al., 2019). The Bafoussam dykes have been dated by K-Ar to the Carnian (Kouankap Nono et al., 2019). In Chad, the transitional gabbro of Doba is dated by Ar-Ar to the Lopingian (Shellnutt et al., 2015). These dykes, attributed to an extensional regime preceding the breakup of Gondwana in Central Africa, exhibit chemical compositions distinct from those of the CL.

Transitional basalts are also present in the CL and have occasionally been dated by K-Ar. In the Bamoun Plateau dating has yielded ages of 51.8 Ma (Moundi et al., 2007) and between 50.8 and 46.5 Ma (Okomo Atouba et al., 2016). In the Mont Bangou area, they have been dated to 44.7–43.1 Ma (Fosso et al., 2005*).* To the south of the Mont Bambouto, at Fotouni*,* they range from 47.13 to 38.70 Ma (Ngongang TchiKoukou et al., 2021). At Bafoussam, they have been dated between 46.97 and 37.84 Ma (Essomba et al., 2022). These basalts represent the oldest known volcanic rocks in the CL.

The transitional dolerites of the MOLB and BFB region have incompatible element contents more similar to those of the transitional basalts of the CL than to those of the Paleozoic dykes. They could therefore be associated with the earliest volcanic manifestations of the CL, which may extend northeastward as far as the Ouaddaï Massif in Chad (Djerossem et al., 2024).

V. Conclusion

This study provides new insights into the magmatic and geotectonic history of the MOLB and BFB, highlighting the diversity of dolerite compositions and their tectonic significance. The geochemical reclassification of dolerites from the literature into IRT, CT, transitional, and alkaline types highlights the complexity of rift-related magmatic and lithospheric processes. Despite these advances, the absence of absolute radiometric ages remains a significant limitation in constraining the precise timing of magmatic events.

Future research should focus on geochronological studies to refine the temporal framework of magmatism in the MOLB and BFB region and to better integrate these findings into the geodynamic evolution of the West and Central African Rift System.

References

[1] Aka, F.T., Hasegawa, T., Nche, L.A., Asaah, A.N.E., Mimba, M.E., Teitchou, I., Ngwa, C., Miyabuchi, Y., Kobayashi, T., Kankeu, B., Yokoyama, T., Tanyileke, G., Ohba, T., Hell, J.V., and Kusakabe, M. (2018). Upper Triassic mafic dykes of Lake Nyos, Cameroon (West Africa) I: K-Ar age evidence within the context of Cameroon Line magmatism, and the tectonic significance, Journal of African Earth Sciences, 141, 49–59. http://dx.doi.org/10.1016/j.jafrearsci.2018.02.001.

[2] Álvaro J.J., Pouclet A., Ezzouhairi H., Abderrahmane Soulaimani A., Bouougri E.H, Imaze A.G., and Fekkak A. (2014). Early Neoproterozoic rift-related magmatism in the Anti-Atlas margin of the West African craton, Morocco. Precambrian Res. 255, Part 1, 433–442. https://doi.org/10.1016/j.precamres.2014.10.008

[3] Asaah A.N.E., Yokoyama T., Iwamori H., Aka F.T., Tamen J., Kuritani T., Usui T., Hasegawa T., and Fozing E.M. (2022). Geochemical composition of dykes along the Cameroon Line (CL): Petrogenesis and similarities with the Central Atlantic Magmatic Province. Geochemistry, vol. 82, issue 2, p. 125865. http://dx.doi.org/10.1016/j.chemer.2022.125865

[4] Béa A., Cochemé J.J., Trompette R., Affaton P., Soba D., and Sougy J. (1990). Grabens d'âge paléozoïque inférieur et volcanisme tholéiitique associé dans la région de Garoua au Nord-Cameroun. Journal of African Earth Sciences, 10(4), 657–667. https://doi.org/10.1016/0899-5362(90)90032-A

[5] Benkhelil J. (1986). Structure et évolution géodynamique du bassin intracontinental de la Bénoué (Nigeria). Thèse Sciences, Université de Nice, France, 226 p.

[6] Bessoles B. and Trompette R. (1980). Géologie de l'Afrique : La chaine panafricaine, zone mobile d'Afrique Centrale (partie Sud) et zone soudanaise. Mémoire BRGM, 92, 397 p.

[7] Bessong M., Hell J.V., Elias S., Susanne F.B., Eyong J.T., Ngos SIII., Nolla J.D., Mbesse C.O., Thierry A., Mfoumbeng M.P., Dissombo Edimo A.N., Ntsama Atangana J., Mouloud B., and Ndjeng E. (2018). Hydrocarbon potential, palynology and palynofacies of four sedimentary basins in the Benue Trough, northern Cameroon. Journal of African Earth Sciences, 139, 73–95. https://doi.org/10.1016/j.jafrearsci.2017.11.012

[8] Brunet M., Dejax J., Brillanceau A., Downs W., Duperon Laudoueneix M., Eisenman V., Flanagan K., Flynn E., Heintz E., Hell J., Jacob L., Jehene Y., Ndjeng E., Mouchelin G., and Pibleam D. (1988). Mise en évidence d'une sédimentation précoce d'âge barrémien dans le fossé de la Bénoué en Afrique Occidentale (bassin du MayoOulo-Léré) en relation avec l'ouverture de l'Atlantique Sud. Comptes Rendus de l'Académie des Sciences, Paris 306(II), 1125–1130.

[9] Cabanis B. and Lécolle, M. (1989). Le diagramme La/10-Y/15-Nb/8: un outil pour la discrimination des séries volcaniques et la mise en évidence des processus de mélange et/ou de contamination crustale. Comptes Rendus de l'Académie des Sciences, Paris, 309, 2023–2029.

[10] Castaing C., Feybesse J. L., Thiéblemont D., Triboulet C., and Chevremont P. (1994). Paleographical reconstruction of the Pan-African / Brasiliano orogen: closure of an oceanic domain or intracontinental convergence between major blocks. Precambrian Research, 69, 327–344. https://doi.org/10.1016/0301-9268(94)90095-7

[11] Coulon C., Vidal P., Dupuy C., Baudin P., Popoff M., Malusk H. I, and Hermitte D. (1996). The Mesozoic to Early Cenozoic Magmatism of the Benue Trough (Nigeria); Geochemical Evidence for the Involvement of the St Helena Plume. Journal of Petrology, 37 (6), 1341–1358. https://doi.org/10.1093/petrology/37.6.1341
[12] Djerossem N.F., Mbassa B.J., Vanderhaeghe O. and Gregoire M. (2024). The Iriba alkaline basalts, an expression of mantle-derived Cretaceous magmatism of the Cameroon-Chad volcanic line along the Central Africa Rift System, 356, 231–248. https://doi.org/10.5802/crgeos.282
[13] Dou, L., Xiao, K., Wang, J. (2023). Petroleum Geology and Exploration of the Bongor Basin. Springer, Singapore, 486 p.
[14] Doumnang Mbaigané J.C. (2006). Géologie des formations néoprotérozoïques du Mayo Kebbi (Sud-Ouest du Tchad) : apport de la pétrologie et de la géochimie : implications sur la géodynamique au Panafricain. Thèse, Université d'Orléans, France, 234 p.
[15] Doumnang Mbaigané J.C., Tekoum L., Rochette P., and Vicat J.P. (2025). The Dolerites of the Léré Region (Southwestern Chad, Africa): Petrography and Geochemical Characterisation. International Journal of Multidisciplinary Research and Publications, 7, 10, pp. 22–32.
[16] Essomba P., Chazot G., Tchuimegnie Ngongang N.B., Agranier A., Kamgang P., Bellon H., Nonnotte P., Wotchoko P., and Badriyo I. (2022). The Bafoussam volcanic series: origin and evolution of the volcanism along the Cameroon volcanic line. *Acta Geochim* 41, 1049–1068. https://doi.org/10.1007/s11631-022-00560-z
[17] Fagny Mefire A., Bardintzeff, J.M., Nkouandou, O.F., Lika Gbeleng, T.A., and Ngougoure Mouansie, S. (2019). Petrology and geochemistry of Hama Koussou dolerite dyke swarms (north Cameroon, central Africa). Journal of Geography, Environment and Earth Science International, 23(3), 1–19. Fosso J., Ménard J.J., Bardintzeff J.M., Wandji P., Tchoua F.M., and Bellon H. (2005). Les laves du Mont Bangou: Une première manifestation volcanique éocène, à affinité transitionnelle de la ligne du Cameroun. Comptes Rendus Geoscience, Paris, 337, 315–325.
[18] Fosso Menkem E., Ngounou Ngatcha B., Ngia N. R., Fuanya C., and Ekodeck G.E. (2024).Tectonic and sedimentary evolution of the Northern Cameroon Cretaceous rift basins: A study of the Babouri-Figuil and Mayo Oulo-Lere basins. Geosystems and Geoenvironment, 3, 100291. https://doi.org/10.1016/j.geogeo.2024.100291
[19] Genik G.J. (1992). Regional framework, structural and petroleum aspects of rift basins in Niger, Chad and the Central African Republic (C.A.R.). Tectonophysics, 213, 169–185. https://doi.org/10.1016/B978-0-444-89912-5.50036-3
[20] Gountié Dedzo M., Klamadji M.N., Zangmo Tefogoum G., Chako-Tchamabé B., Asaah A., and Tchameni R. (2023). Major, trace elements and Sr–Nd–Pb isotopes systematics of mafic dykes from the Figuil (northern Cameroon) and Léré (southwestern Chad) areas, Geological Journal, 1–27. https://doi.org/10.1002/gj.4892
[21] Guiraud R., Bellion Y., Benkhelil J., and Moreau C. (1987). Post-Hercynian Tectonics in Northern and Western Africa. Geology Journal, 22, 433–466. https://doi.org/10.1002/gj.3350220628
[22] Guiraud R., Binks R. M., Fairhead J. D. and Wilson M. (1992). Chronology and geodynamic setting of Cretaceous-Cenozoic rifting in West and Central Africa. Tectonophysics, 213, 227–234. https://doi.org/10.1016/0040-1951(92)90260-D
[23] Guiraud R. and Maurin J.C. (1992). Early Cretaceous rifts of Western and Central Africa: an overview. Tectonophysics, 213, 153–168. https://doi.org/10.1016/0040-1951(92)90256-6
[24] Guiraud R. and Bellion Y. (1995). Late Carboniferous to Recent Geodynamic Evolution of the West Gondwanian, Cratonic, Tethyan Margins. In: Nairn, A., Dercourt, J. and Vrielynck, B., (Eds), The Ocean Basins and Margins, 8, The Tethys Ocean, 101–124. https://doi.org/10.1007/978-1-4899-1558-0_3
[25] Holm P.E. (1985). The geochemical fingerprints of different tectonomagmatic environments using hygromagmatophile element abundances of tholeiitic basalts and basaltic andesites. Chemical Geology, 51, 303–323. https://doi.org/10.1016/0009-2541(85)90139-1
[26] Irvine T.N. and Baragar W.R.A. (1971). A guide to chemical classification of the common volcanic rocks. Canadian Journal of Earth Sciences, 8, 523–548. https://doi.org/10.1139/e71-055
[27] Isseini M. (2011). Croissance et différenciation crustales au Néoprotérozoïque Exemple du domaine panafricain du Mayo Kebbi au Sud-Ouest du Tchad. Thèse, Univ Nancy I, 340 p.
[28] Jacobs L.L., Congleton J.O., Brunet M., Dejax J., Flynn L., Hell J.V., and Mouchelin G. (1988). Mammal teeth from the cretaceous of Africa. Nature 336 (6195), 158e160.
[29] Klamadji M.N., Gountié Dedzo M., Tchameni R., and Dawaï D. (2020). Petrography and geochemical characterization of dolerites from Figuil (Northern Cameroon) and Léré (southwestern Chad). International Journal of Geosciences, 11(7), 459–482. https://doi.org/10.4236/ijg.2020.117023
[30] Klamadji M.N., Gountié Dedzo M., Tchameni R., Hamadjoda D.D., Biakan à Nyotok P. C., and Onana G. (2021). Fractional crystallization and crustal contamination of doleritic and trachytic dykes crosscutting the Cretaceous sedimentary basins from Figuil (North Cameroon) and Léré (South-Western Chad): geodynamic implications. Journal of Geoscience and Environment Protection, 9(12), 190–210. https://doi.org/10.4236/gep.2021.912012
[31] Klamadji M.N., Tekoum L., Baïssemia R.G., Merlin Gountié Dedzo M., Djérossem N.F., Béninga L.F., and Didi D. (2025). Geochemical Characterizations of the Hypovolcanic Formations of the Pan-African Basement and the Cretaceous Sedimentary Basins of Figuil (North Cameroon) and Léré (South-West Chad): Petrogenetic and Geodynamic Implication of the Pan-African Range of Central Africa (CPAC). International Journal of Geosciences, 16, 127-153. doi: 10.4236/ijg.2025.162007.
[32] Kouankap Nono G.D., Wotchoko P., Ganno S., Njinchuki D. and Nzenti J.P. (2013). Petrochemical Characterization of Two Distinct Types of Dolerites from Bafoussam Area, West Cameroon," International Journal of Geosciences, 4(8), 1131–1144. https://doi.org/10.4236/ijg.2013.48107
[33] Kouankap Nono G. D., Wotchoko P., Tanko Njiosseu E. L., Ganno S., Tene Djoukam J. F., Seplong Y., and Nkouathio D. G. (2019). A Gondwana pre-break up related magmatism in Bafoussam area, West Cameroon: Source characteristics and 40Ar/39Ar geochronology. International Journal of Advanced Geosciences, 7(1), 23–30.
[34] Keutchafo Kouamo N.A., Tchatptchet T.D., Ngueguim Tezanou A.L., Simeni Wambo N.A., Tchouankoue J.P., and Cucciniello C. (2019). Petrogenesis of basaltic dikes from the Manjo area (Western Cameroon): Insights into the Paleozoic magmatism at the northern margin of the Congo craton in Cameroon. Arab. J. Geosci., 12:281.
[35] Lasserre M., Baubron J.C., and Cantagrel J.M. (1977). Existence d'une couverture non plissée d'âge paléozoïque inférieur, au sein de la zone mobile de l'Afrique centrale: Age K/Ar des formations de type Mangbai. C. R. Acad. Sci., Paris. D, 284: 2667-2670.
[36] Le Bas M.J., Le Maitre R.W., Streckeisen A., and Zanettin B. (1986). A chemical classification of volcanic rocks based on the total alkali–silica diagram. Journal of Petrology, 27, 745–750. https://doi.org/10.1093/petrology/27.3.745
[37] Lee C.-T.A., Luffi P., Plank T., Dalton H., and Leeman W.P. (2009). Constraints on the depths and temperatures of basaltic magma generation on Earth and other terrestrial planets using new thermobarometers for mafic magmas. Earth Planet Sci. Lett. 279, 20–33.
[38] Lemdjou Y.B., Tchaptchet Tchato D., Huan L, Whattam S. A., Soh Tamehe L., Elatikpo S. M., and Madayipu N. (2022). Cambrian mafic magmatism in the Kékem area, NW edge of the Adamawa-Yadé domain, Central African Fold Belt: Implications for Western Gondwana dynamics. Precambrian Research, vol. 380, p. 106840. https://doi.org/10.1016/j.precamres.2022.106840
[39] Lu Y., Liu J., Dou L., Guo Z., Xiao K., Hu Y., and Du Y. (2009a). Geochemistry and petrogenesis of volcanic rocks from Chad basins, Africa. Acta Petrol. Sin. 25 (1), 109–123.
[40] Lu Y., Liu J., Dou L., Guo Z., Xiao K., Hu Y., Du Y., and Meng F. (2009b). K-Ar and 39Ar40Ar geochronology of basalts from the Chad basins, Africa and its geodynamics setting. Acta Petrol. Sin. 83 (8), 1125–1133
[41] Maluski H., Coulon C, Popoff M., and Baudi, P. (1995). 40Ar/39Ar chronology, petrology and geodynamic setting of Mesozoic to early Cenozoic magmatism from the Benue Trough, Nigeria. Journal of the Geological Society of London 152, 311–326.
[42] Manga Owona G.W., Bessong M., Mioumnde A.P., Mbesse C.O., Bapowa L.C., Kusi Ngum M.M.A., Meyin A., Ekomane P.E., and Samankassou E. (2023). Litho-bio-stratigraphy model and palaeoenvironments of the Babouri-Figuil basin (NE Cameroon): a lacustrine/fluvial/deltaic setting associated to the Benue trough (Nigeria). J. Afr. Earth Sci. 207 (1), 105021. https://doi.org/10.1016/j.jafrearsci.2023.105021.

[43] Maurin J.C. and Guiraud R. (1989). Relation entre tectonique et sedimentation dans les bassins barrémo-aptiens du Nord Cameroun. C.R. Acad. Sci. Paris, t. 308 (II), 787–792.
[44] Maurin J.C. and Guiraud, R. (1990). Relationships between tectonics and sedimentation in the Barrémo-Aptian intracontinental basins of Northern Cameroon. Journal of African Earth Sciences, 10 (1-2), 331–340. https://doi.org/10.1016/0899-5362(90)90064-L
[45] Maurin J.C. and Guiraud, R. (1993). Basement control in the development of the early cretaceous West and central African Rift System. Tectonophysics, 228, 81–95. https://doi.org/10.1016/0040-1951(93)90215-6
[46] Miyashiro A. (1975). Classification, Characteristics, and Origin of Ophiolites. Journal of Geology, 83 (2), 249–281.
[47] Moundi A., Wandji P., Bardintzeff J-M., Ménard J-J., Atouba L.C.O., Mouncherou O.F., Reusser É., Bellon H., and Tchoua F.M. (2007). Les basaltes éocènes à affinité transitionnelle du plateau Bamoun, témoins d'un réservoir mantellique enrichi sous la ligne volcanique du Cameroun. Compt Rendus Geosci 339,396–406.
[48] Ndjeng E. (1992). Etude de la sédimentologie et du modèle d'évolution géodynamique de deux bassins du Crétacé inférieur du Nord Cameroun : Babouri-Figuil et Mayo Oulo- Léré. Thèse, Université de Yaoundé, Cameroun, 311 p.
[49] Ngo Elogan Ntem, J., Ngounfack Tiokeng V, Toyama R, Berinyuy Konglim Y., Takoi J.F., Togoum N., Ngnotue T., and Tchouatcha M. S. (2024). Geochemical constrains for unravelling the condition of sedimentation, provenance, paleoclimate variation, and metallogenic implication of the cretaceous deposits of Mayo Oulo Basin (North Cameroun, Africa). Solid Earth Sciences, 9, 100188. https://doi.org/10.1016/j.sesci.2024.100188
[50] Ngongang Tchikankou L.N., Kamgang P., Chazot G., Agranier A., Bellon, H., Nonnotte P., Tchuimegnié Ngongang N.B., and Kwekam M. (2020). Mantle source evolution beneath the Cameroon volcanic line: geochemical and geochronological evidences from Fotouni volcanic series, Western Cameroon. *Arab J Geosci* 13, 1301. https://doi.org/10.1007/s12517-020-06333-3
[51] Ngounouno I., Guiraud R., Déruelle B., and Vicat J.P. (2001). Magmatismes tholéiitiques et alcalins des demi-grabens crétacés de Mayo-Oulo-Léré et de Babouri-Figuil (Nord du Cameroun-Sud du Tchad) en domaine d'extension continentale. Comptes Rendus de l' Académie des Sciences, Série IIa : Earth and Planetary Science, 333, 201–207. https://doi.org/10.1016/S1251-8050(01)01626-3
[52] Nkouandou O.F., Bardintzeff J.M., Mahamat O., Fagny Mefire A., and Ganwa A.A. (2017). The dolerite dyke swarm of Mongo, Guéra Massif (Chad, Central Africa): Geological setting, petrography and geochemistry. Open Geosciences, 9, 138–150. https://doi.org/10.1515/geo-2017-0012
[53] Nkouandou O.F., Bardintzeff J.M., Fagny Mefire A., Koromi A.B., Mahamat O., and Ngougoure M.S. (2022). Geodynamic framework of the magmatic activity of Cretaceous Léré basin (Southwestern Chad, Central Africa). Journal of African Earth Sciences, 194(1), 104630. https://doi.org/10.1016/j.jafrearsci.2022.104630
[54] Nyangono Abolo A.J., Ngos III S., Balla Ondou, A.D., Garcia B., Fernanda- Sarmiento M., Mbesse C.O., Abolo G.M., Eloung Nna M.D., Nkenfack A.E., Ndjeng E., and Qiang J. (2014). Geochemical characterization and mineralogy of Babouri-Figuil oil shale, North Cameroon. J. Surf. Eng. Mater. Adv. Technol. 4, 359–368.
[55] Okomo Atouba C.L., Chazot G., Moundi A., Agranier A., Bellon H., Nonnotte P., Nzenti J.P, and Kankeu B. (2016) Mantle beneath the Cameroon Volcanic Line: geochemistry and geochronology of the Bamoun plateau mafic rocks. Arabian Journal of Geosciences, 9, 1–12. https://doi.org/10.1007/s12517-015-2285-6
[56] Pearce J.A. (2008). Geochemical fingerprinting of oceanic basalts with applications to ophiolite classification and the search for Archean oceanic crust. Lithos, 100, 14–48. https://doi.org/10.1016/j.lithos.2007.06.016
[57] Pearce J.A. and Cann J.R. (1973). Tectonic Setting of Basic Volcanic Rocks Determined Using Trace Element Analyses. Earth and Planetary Science Letters, 19, 290–300. https://doi.org/10.1016/0012-821X(73)90129-5
[58] Pearce J.A. (1996). A User's Guide to Basalt Discrimination Diagrams. In: Wyman, D.A., Ed., Trace Element Geochemistry of Volcanic Rocks: Applications for Massive Sulphide Exploration, Geological Association of Canada, Short Course Notes, 12, 79–113.
[59] Rooney T.O. (2010). Geochemical evidence of lithospheric thinning in the southern Main Ethiopian Rift. Lithos, 117, 33–48. https://doi.org/10.1016/j.lithos.2010.02.002
[60] Rudnick R.L. and Gao S. (2004). Composition of the continental crust. In: Holland, H.D., and Turekian, K.K. (Eds.), Treatise on Geochemistry, 3, 1–64.
[61] Schwoerer P. (1965) Carte Géologique de Reconnaissance à L'échelle 1/500000. Notice Explicative sur la Carte Garoua-Est. Direction des Mines et de la Géologie du Cameroun, Yaoundé 49 p.
[62] Shellnutt J.G., Lee T.Y., Yang C.C., Hu S.T., Wu J.C., Wang K.L, and Lo C.H. (2015). Late Permian mafic rocks identified within the Doba basin of southern Chad and their relationship to the boundary of the Saharan Metacraton. Geological Magazine, 1, 1–12. https://doi.org/10.1017/S0016756815000217
[63] Smith E.I., Sanchez A., Walker J.D., and Wang K. (1999). Geochemistry of mafic magmas in the Hurricane Volcanic Field, Utah: implications for small- and large-scale chemical variability of the lithospheric mantle. The Journal of Geology, 107(4), 433–448. http://dx.doi.org/10.1086/314355
[64] Sun S. and McDonough W. (1989). Chemical and isotopic systematics of ocean basalts: implications for mantle composition and processes. Geological Society of London Special Publication, 42, 313–345. http://dx.doi.org/10.1144/GSL.SP.1989.042.01.19
[65] Tchaptchet Tchato, D., Wambo Simeni, N.A., Keutchafo Kouamo, N.A., Tchouankoue, J.P., and Cucciniello, C. (2017). Geology, mineralogy and geochemistry of the Kekem dyke swarm (Western Cameroon): insights into Paleozoic-Mesozoic magmatism and geodynamic implications. Compt. Rendus Geosci, 349, 175–185.
[66] Tchouatcha M.S., Azinwi Tamfuh P., Sobdjou Kemteu C., Mbesse C.O., and Ngnotue T. (2021a). Provenance, palaeoweathering and depositional environment of the cretaceous deposits from the Babouri-Figuil and Mayo Oulo-Lere basins (North-Cameroon) during the Southern Atlantic opening: geochemical constraints. Journal of African Earth Sciences, 174, 104052. https://doi.org/10.1016/j.jafrearsci.2020.104052.
[67] Tchouatcha M.S., Sobdjou Kemteu C., Mbesse C.O., Ouandji Sime L.L., Miyemeck Ngonlep V.T., and Tchounang Kouonang S. (2021b). Mechanisms of sedimentation in lacustrine environment of Babouri-Figuil and Mayo Oulo-Lere basins deposits (North Cameroon) during the Southern Atlantic opening: sedimentary structures and geochemistry constraints. Arabian Journal of Geosciences, 14(6), 450. https://doi.org/10.1007/s12517-021-06763-7.
[68] Toteu S.F., Penaye J., and Poudjom Djomani Y.H. (2004). Geodynamic evolution of the Pan-African belt in Central Africa with special reference to Cameroon. Canadian Journal of Earth Sciences, 41, 73–85. https://doi.org/10.1139/e03-079
[69] Vicat J.P., Ngounouno I., and Pouclet, A. (2001). Existence de dykes doléritiques anciens à composition de tholéiites continentales au sein de la province alcaline de la ligne du Cameroun. Implication sur le contexte géodynamique. C. R. Acad. Sci. Paris 332, 243–249.
[70] Wacrenier P. (1962). Carte géologique de reconnaissance des Etats d'Afrique Equatoriale. Feuille NC-33 SO E-53 SE O-54 (Moundou) au 500 000ème. IRGM, Brazzaville.
[71] Wang K., Plank T., Walker J.D., and Smith E.I. (2002). A mantle melting profile across the Basin and Range, SW USA. Journal of Geophysical Research, 107(b1). https://doi.org/ 10.1029/2001JB000209
[72] Wang K., Plank T., Walker J.D., and Smith E.I. (2002). A mantle melting profile across the Basin and Range, SW USA. Journal of Geophysical Research, 107(b1). https://doi.org/ 10.1029/2001JB000209
[73] Wilson M., Guiraud R., Moreau C., and Bellion Y.J.C. (1998). Late Permian to Recent Magmatic Activity on the African-Arabian Margin of Tethys. In: Macgregor, D.S., Moody, R.T.J. and Clark-Lowes, D.D. (Eds.), Petroleum Geology of North Africa, Geological Society. London Special Publications, 132, 231–263. https://doi.org/10.1144/GSL.SP.1998.132.01.14
[74] Winchester J.A., and Floyd P.A. (1977). Geochemical magma type discrimination: application to altered and metamorphosed basic igneous rocks. Earth and Planetary Science Letters, 28(3), 459–469. https://doi.org/10.1016/0009-2541(78)90050-5
[75] Wolff J.P. (1964). Carte géologique de la République du Tchad au 1/1 500 000. B.R.G.M, Paris.